Monitoring of the creep and the relaxation behaviour of concrete since setting time, part 2 : tension

Brice Delsaute, Stéphanie Staquet, Claude Boulay

Monitoring of the creep and the relaxation behaviour of concrete since setting time, part 2 : tension

SSCS 2012 Numerical Modeling Strategies for Sustainable Concrete Structures
Aix-en-Provence, France
May 29-June 1, 2012

B. Delsaute[1], S. Staquet[1], C. Boulay[2]

[1]*ULB (Université Libre de Bruxelles), BATir Department – Brussels, Belgium*
[2] *IFSTTAR-Paris, Paris East University, France*

1. Introduction

Nowadays, the construction phases of modern concrete structures become more and more complex. Consequently, it is important to have a knowledge in depth of the early age behaviour of concrete, what will influence all the service life of the concrete structures. Even though the mechanical behaviour of hardened concrete can usually be correctly predicted; it is not always the case for the early age behaviour of concrete, when the mechanical properties change rapidly in function of the advancement of the hydration reaction. Among all the usual parameters (strengths, E-modulus…) needed for the design of the concrete structures, creep and relaxation in tension and in compression must also be taken into account. For example, in the design of a concrete dam, Slowik [1] showed that at early age, the relaxation phenomenon was responsible for a decrease of 70% of the thermally induced stresses in the structure.

A partnership between IFSTTAR and ULB allowed joined experimental tests on the same ordinary concrete in order to investigate the early age mechanical behaviour since setting time. Besides the usual determination of the instantaneous mechanical properties, this paper (part 1 & 2) presents an experimental methodology using two different test rigs enabling a monitoring of the stiffness, the creep or the relaxation of a concrete sample since setting time. Tension and compressive tests have been carried out on a revisited Temperature Stress Testing Machine (TSTM) at ULB [2][3] and are mainly presented in this part while compressive tests, carried out on another test rig called BTJASPE designed at IFSTTAR, have been presented in the first part.

A revisited TSTM system was developed in the laboratory of civil engineering at ULB for testing concrete in tension or in compression since setting time under free and restraint conditions. The TSTM consists of an electromechanical testing setup, where one end of the specimen is restrained by a steel head and the displacement of the other end is controlled by a motor moving the other steel head. The shape of the mould is a dog-bone. The Young's modulus, the creep or the relaxation of the sample can be monitored at early age by means of automatic cyclic loadings applied at regular intervals in tension or in compression. As in addition to the creep and elastic deformations, thermal and shrinkage deformations must also be known, a dummy mould was realized for the measurement of the thermal and free shrinkage deformations. A thermal regulation allowing the control of the sample's temperature was included in the revisited TSTM system as well as a couple of displacement sensors without contact allowing the start of the measurement since setting time.

For all the tests, rheological models are used for the description of the experimental set of data. In addition to the presentation of the results obtained in tension, the purpose of this part is to discuss the question of the equivalence between the early age creep and relaxation behaviour of concrete in tension and in compression for a typical ordinary concrete under isothermal (20°C) and sealed conditions. Finally, the creep recovery in tension is studied and discussed.

2. Test setup

2.1. Tested concrete description

The mixture proportions of the ordinary concrete under focus are given in Table 1. The water to cement ratio is equal to 0.54. More information about mechanical properties is given in part 1.

.

Components	Mass (kg /m^3)
CEMI 52.5 N PMES CP2	340
Sand (Bernières 0/4)	739
Gravel (Bernières 8/22)	1072
Total water	184

Table 1 - Mixture proportions of the concrete

2.2. Experimental tools

A revisited TSTM system was developed (since 2006) in the laboratory of civil engineering at the ULB for testing concrete since setting time under free and restraint conditions. For this purpose, a testing machine, a Walter+Bay LFMZ 400 kN electromechanical testing setup, has been revisited. The machine is totally programmable and controlled (force and displacement of each sensor) by computer. The machine is composed by a fixed steel head, a central unidimensional part and a moving end (Figure 2). The moving end is controlled by a motor moving the steel head. The transition area between the ends and the central part is characterized by a rounded shape in order to minimize a possible stress concentration and the risk of premature cracking in this zone. In the central part where the measurements of the displacements are taken, the stress field is assumed to be homogenous.

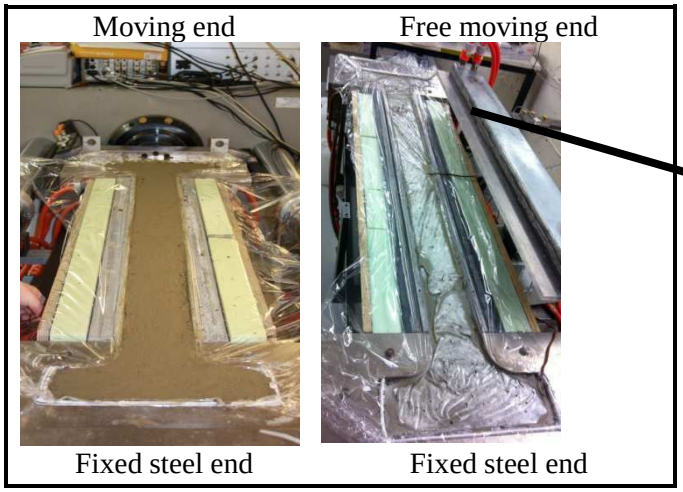

Figure 2 – a couple of moulds with different boundary conditions

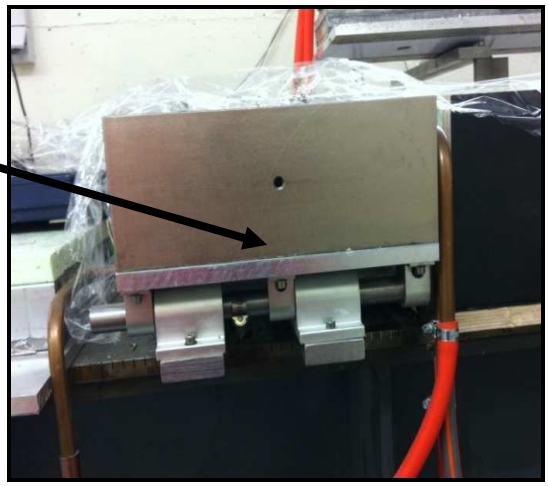

Figure 1 – Dummy mould : free moving end thanks to ball bearings

In addition to the creep and elastic deformations, thermal and shrinkage deformation must also be known. For this purpose, a dummy mould was realized for the measurement of the thermal and free shrinkage deformations. This mould has exactly the same geometry as the first one. The only difference is the total free movement of one of the ends (Figure 1).

The shape of the mould is a dog-bone. The dimensions of the cross section are 100x100 mm² in the central part and 300x100 mm² at the ends. The total length of the straight part is 1000 mm. With these dimensions, it is possible to realize tests for concrete with a maximal aggregate size of 20 mm. The fresh concrete is cast inside the mould up to a level of 100 mm. One T type thermocouple is placed in the middle of the sample during the casting, at each end and at mi-length of the central part of the mould. The temperature of the sample is controlled by a flow of a specific liquid for thermal

regulation circulating on all the sides of the specimen. A plastic sheet is placed, before casting, in the mould to ensure sealed conditions. Moreover, the plastic sheet helps also to reduce, with the presence of Teflon, the friction between the sample and the mould. The walls of the mould are made of aluminum (Figure 3) which was chosen for its high thermal conductivity (237 W/m.K) and its low density (2700 kg/m³). The deflection of the mould is very limited (+/-2mm) and the isothermal conditions are ensured thanks to a fast heat transfer with the zinc boxes. A specific liquid for thermal regulation flows inside zinc boxes beams which are placed all around the central part and on the ends and under them. Each box is independent and has its own water input and output system. A thermal insulation limits exchanges with the ambient environment. The equipment is located in an air-conditioned room with a control system of the temperature and the humidity.

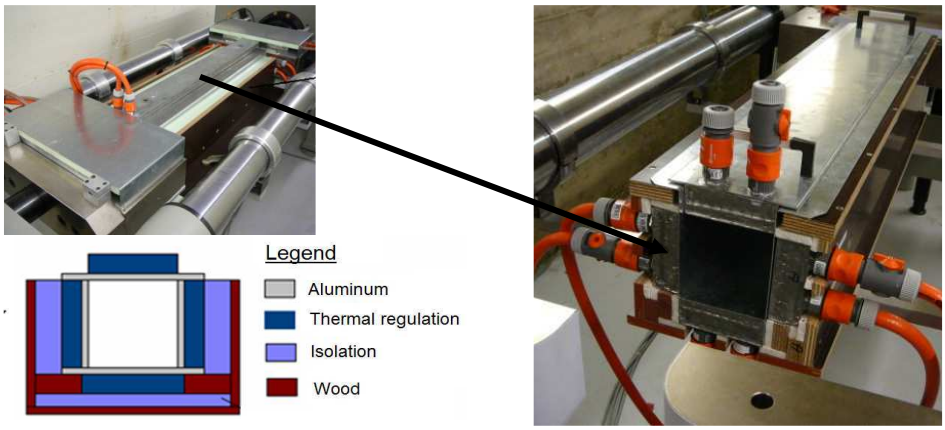

Figure 3 - Thermal insulation

Displacements in the central part are recorded by Foucault current's sensors (contact free sensors). Sensors have an accuracy of 0.014 µm. The displacement sensors of displacement are placed on invar supports which are fixed on a rigid frame made of steel bars externally supported by the TSTM (Figure 4). The distance between both sensors is 750 mm (where the stress field is homogeneous in the sample). Invar rods are anchored in the concrete at a depth of 50 mm. The link between the concrete displacement and the sensor is then assured. These invar rods are characterized by a low dilatation coefficient limiting the effect of ambient temperature on the deformations measurement. They are kept in their initial position thanks to a brass ring before the beginning of the test. These sensors have two advantages. Firstly, the absence of contact between the sensors and the mould avoids measurement artifacts. Secondly, an instantaneous volt conversion in micrometer of the sensors allows piloting the TSTM system with the displacement directly measured in concrete.

Figure 4 - displacement sensors in the central part of the specimen

The horizontality of the TSTM device is an advantage for the efficiency of the casting. Moreover, sensors are well anchored at mid-height and not in the superficial layer of the sample, what could have induced an error by a possible different mechanical behavior between the core layer and the superficial layer characterized by a lower density in aggregates than the one of the core layer.

2.3. Protocol of loadings

The system is controlled in displacement (measured in the straight part of the concrete sample or at the end of the moving steel head) and in force. The direct measurement of the evolution of the Young's modulus, the creep and the relaxation can be carried out. The start of the tests has been choosen at the end of the setting time [4][5]. This time is determined thanks to a device called FreshCon allowing the determination of the setting time on basis of ultrasonic measurements [6].

2.3.1. Relaxation test

Figure 5 introduces the protocol of loadings for the study of the relaxation phenomena. Firstly, the sample is loaded. The Young's modulus measurement is done as follows: for every cycle of loading, the moving end is controlled by the displacement sensor at the end of the moving steel head and the increase of the loading. The increase of the loading is carried out at constant speed (between 1 and 5 µm/s), the value of the speed depends on the stiffness of the concrete, the concrete strength at the age of loading and the type of loading (compression or tension) because the sample is loaded at 20% of the strength/stress ratio in compression and at 40% of the strength/stress ratio in tension.

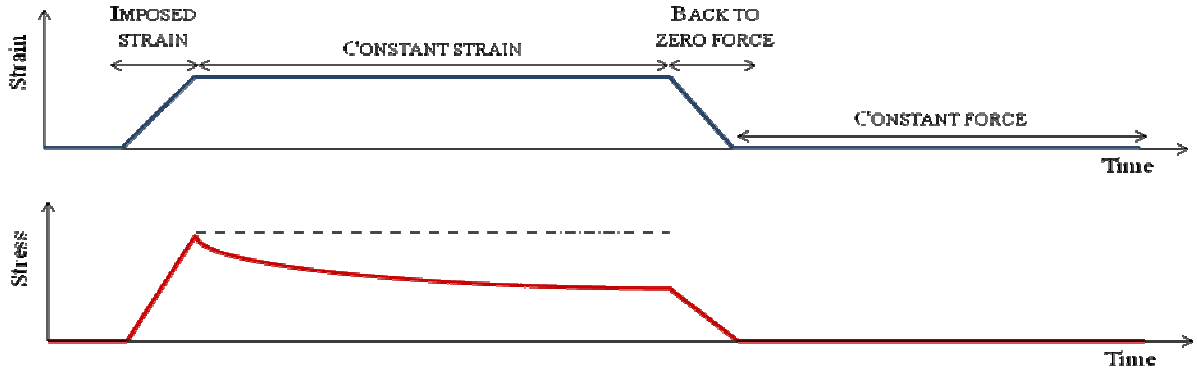

Figure 5 - relaxation cycle in tension

Secondly, a constant strain in the sample is imposed thanks to a real time subtraction between the strain of the specimen in the TSTM and the dummy specimen in the companion (passive) mould. The recorded displacements by sensors without contact are noted S1, S2 in the mould 1 (TSTM) and S3, S4 in the mould 2. The initial distance between the sensors is equal to 750 mm. It allows piloting the TSTM system on basis of the mechanical parameters excluding the free deformations due to thermal variations ε_{th} and due to shrinkage ε_{sh}. So, the direct measurement of the elastic ε_e and creep ε_c strains or the relaxation stresses is possible with the simultaneous use of the first and the second mould (Table 2).

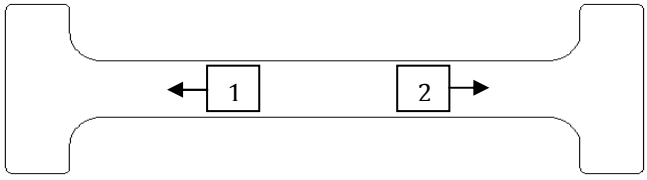	Mould 1: $\frac{S1+S2}{750\ mm} = \varepsilon_e + \varepsilon_c + \varepsilon_{th} + \varepsilon_{sh}$
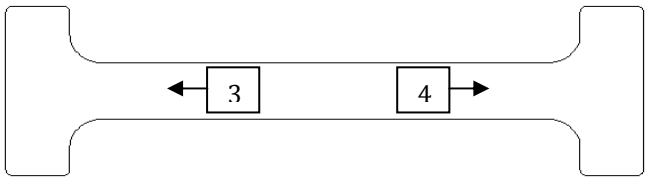	Mould 2: $\frac{S3+S4}{750\ mm} = \varepsilon_{th} + \varepsilon_{sh}$
TSTM device is controlled by (S1+S2)-(S3+S4) which corresponds to creep and elastic strains.	

Table 2 – Strain measurements for each mould

The sample is then unloaded and the moving end is moved backwards to a null force for a period of 24

mn. Recordings are taken during the cycles. The Young's modulus is computed from measurements taken in concrete in the straight part of the sample during each loading cycle. The strains in the straight part are not restraint by the shape and the walls of the mould (friction is supposed to be very low between Teflon® and plastic sheet). These displacement measurements can then be directly used to compute the Young's modulus. The stresses relaxation is computed during the plateau of deformation.

2.3.2. Creep test

Figure 6 introduces the protocol of loadings for the study of the creep phenomena. Firstly, the sample is loaded at 40% of the strength/stress ratio in tension as for the relaxation test in tension. Secondly, a constant force in the sample is imposed during 5 mn. The sample is then unloaded and the moving end is moved backwards to a null force for a period of 24 mn. Recordings are taken during the cycles. The Young's modulus is computed from measurements taken in concrete in the straight part of the sample during each loading cycle. The creep strain is computed during the plateau of force. The creep recovery is computed during the plateau at null force.

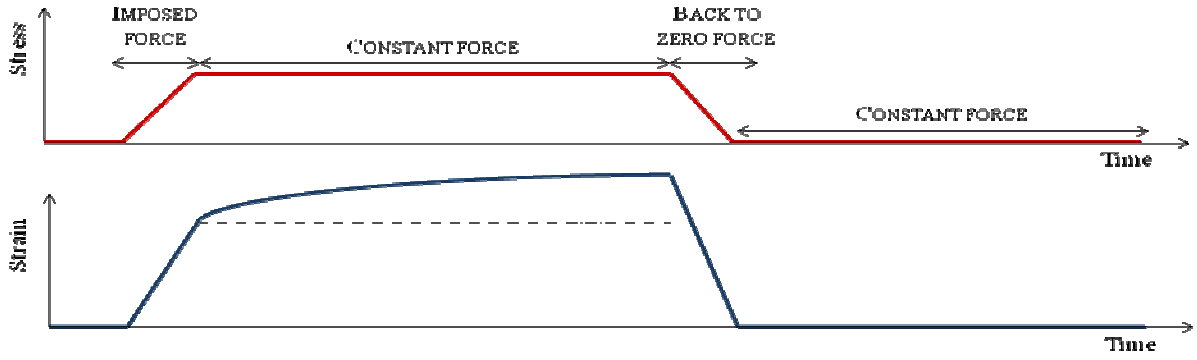

Figure 6 - creep cycle

3. Results and discussions

One tensile creep test and one relaxation test in tension and compression are presented here.

3.1. Relaxation test

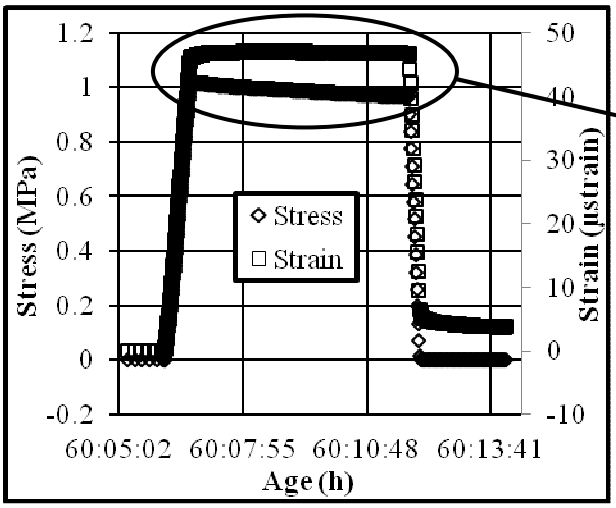

Figure 7 – Typical relaxation cycle in tension

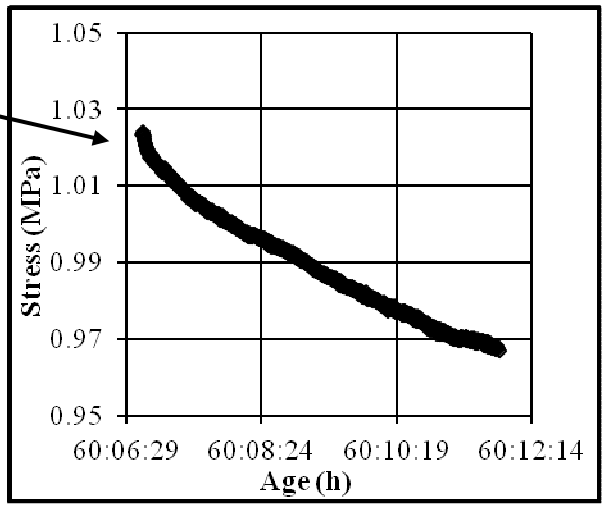

Figure 8 – Zoom on the relaxation stresses during one cycle

A typical relaxation record is presented in Figure 7 and Figure 8. The age of the concrete is called t. The stress evolution is measured continuously. At any cycle, named i, the relaxation is counted as soon as the plateau is reached; this moment is called t_{0i}. The stress $\sigma(t,t_{0i})$ is then recorded whereas a constant strain ε_{0i} is applied. The ratio in Equation 1 is defined as the stiffness. The specific relaxation R^* is defined as this stiffness diminished of the initial stiffness at t_{0i} (see Equation 2).

$$R(t,t_{0i}) = \frac{\sigma(t,t_{0i})}{\varepsilon_{0i}} \quad (1)$$

$$R^*(t,t_{0i}) = R(t,t_{0i}) - R(t_{0i},t_{0i}) = R(t,t_{0i}) - E(t_{0i}) \quad (2)$$

The whole test duration was 68 hours. The duration of each cycle is around 30 minutes. The loading is fixed to a value equal at any time to a percentage of 40 % of the tensile strength and to a percentage of 20 % of the compressive strength. Figure 9 shows an uniaxial rheological model, proposed by Bazant [7], which is used to fit the observed stiffness of each cycle (relaxation function).

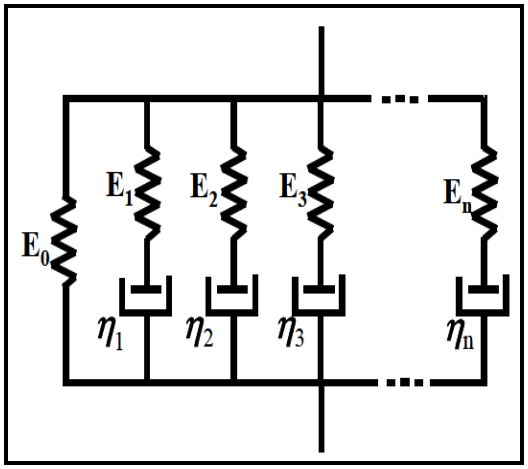

Figure 9 - Multiple Maxwell's chains

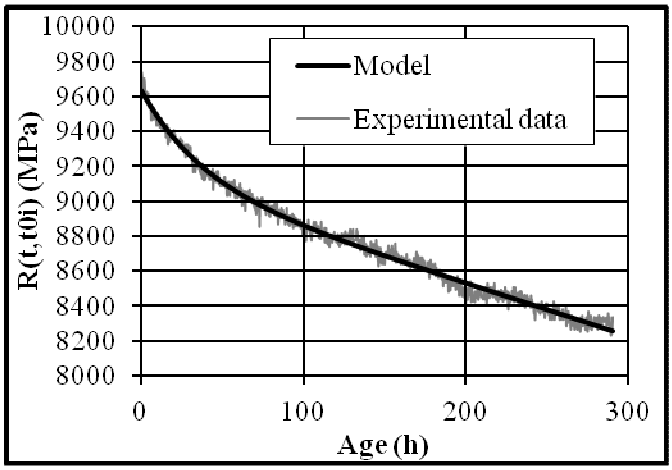

Figure 10 - Relaxation function modeling for the 5th cyle in tension with multiple Mawell's chains model

Relaxation function can be develop in Dirichlet's series expansion [7]:

$$R(t,t_{0i}) = E_0(t_{0i}) + \sum_{\mu=1}^{N} E_\mu(t_{0i}).e^{\frac{t_{0i}-t}{\tau_\mu}} \quad (3)$$

$$\tau_\mu = \tau_1.10^{1-\mu} \ (\mu = 1, \ldots, N) \quad (4)$$

$$\eta_\mu(t) = \tau_\mu.E_\mu(t) \quad (5)$$

With τ_μ= characteristic time
E_μ= μ^{th} spring of the multiple Maxwell's chains
η_μ= μ^{th} dashpot of the multiple Maxwell's chains
t_{0i}= time when the plateau is reached for the i^{th} cycle

The characteristic time τ_1 is supposed as constant and has to be optimized for the best fit. A value of 12 seconds was considered for τ_1. Three Maxwell's chains are used for the modeling of the experimental data of the relaxation test. The least and square method is used to define the value of the different parameters of the rheological model. Figure 10 shows the very good agreement between the modelling of the relaxation function and the experimental data.

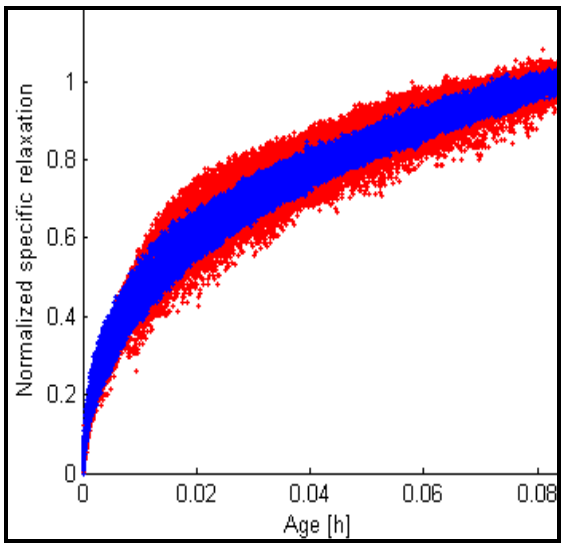

Figure 11 - The specific creeps are normalized by their value at 5 mn.

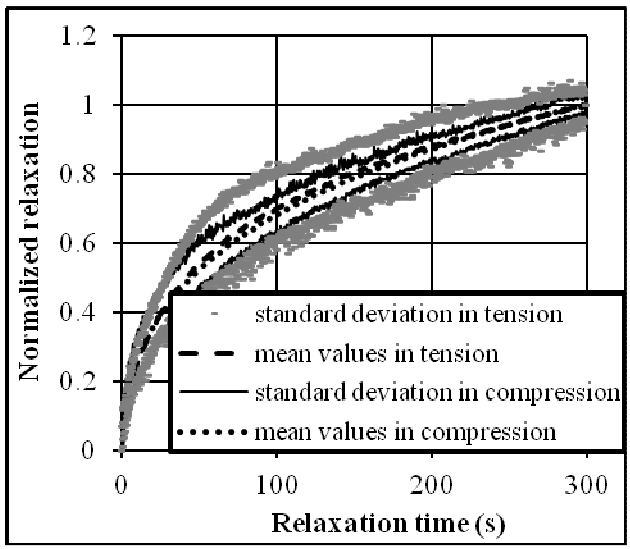

Figure 12 – Mean values of the normalized relaxation in tension and compression between +/- standard deviation fitted by rheological model.

As shown in part 1, the relaxation function or stiffness curves for each cycle can be normalized by the value reached at the end of the plateau and superimposed for looking at the evolution of the kinetics in function of the time. In order to do this, all stiffness curves normalized for the cycle carried out in tension and compression are plotted in Figure 11 . The standard deviation of all these relaxation curves is very low, what shows that the kinetics of the relaxation in tension and compression are independent of the time at early age. No significant difference between tensile and compressive relaxation curves can be observed. The mean values and the standard deviation in tension and in compression are plotted in the Figure 12. The deviations in tension are higher than those in compression because of the lack of accuracy of the measurements related to very small values of loadings applied in tension (ratio of 5 between compressive and tensile loadings) due to the presence of a noise on the measurements of very low amplitude. In part 1, results in compression are compared with another device (BTJASPE). It was shown that the results are perfectly superimposed and then validate the results for both machines. For short durations of loadings (5 mn) and low stress strength ratio, the kinetics of the relaxation in tension and in compression are similar.

3.2. Creep test

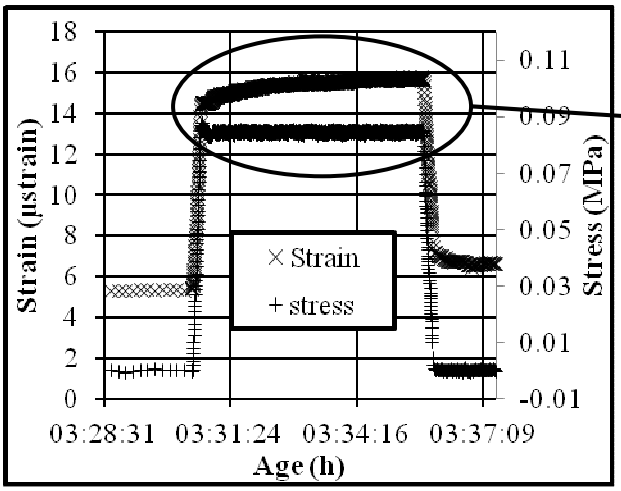

Figure 13 – Typical creep cycle

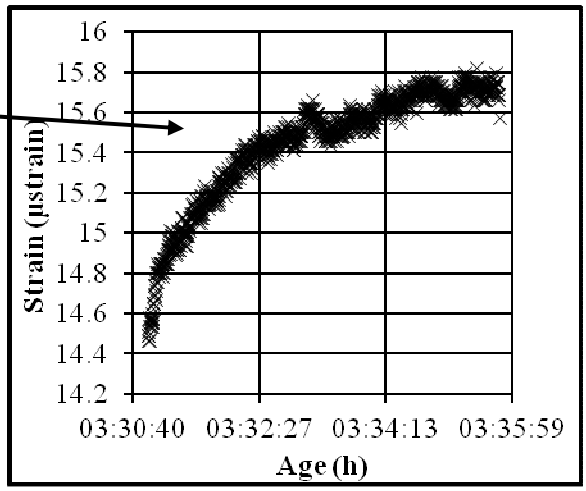

Figure 14 – Zoom on the creep strains during one cycle

A typical creep record is presented in Figure 13 and Figure 14. The sample strain, $\varepsilon(t)$ is measured continuously. At any cycle, named i, the creep is counted as soon as the plateau is reached. This moment is called t_{0i}.

The whole test duration was 72 hours. The duration of each cycle is around 30 minutes. The loading is fixed to a value equal to 40 % of the tensile strength and 20 % of the compressive strength. Figure 9 shows an uniaxial Dirichlet's creep model which is used to fit the observed relaxation data of each cycle. In case of creep, a multiple Kelvin-Voigt's chains (Figure 15) is used to fit the observed creep data of each cycle as it was suggested by Bazant [8]. The creep $J(t,t_{0i})$ can be computed for each cycle during the loading plateau. The mathematical resolution (Dirichlet's series expansion) of the rheological model gives the relation between the creep function and the different parameters of the rheological model (Equation 6).

$$J(t,t_{0i}) = \frac{1}{C_0(t_{0i})} + \sum_{i=\mu}^{N} \frac{1}{C_\mu(t_{0i})}\left(1 - e^{-\frac{t-t_{0i}}{\tau_\mu}}\right) \quad (6)$$

$$\tau_\mu = \tau_1 . 10^{1-\mu} \ (\mu = 1, \ldots, N) \quad (7)$$

$$\eta_\mu(t) = \tau_\mu . E_\mu(t) \quad (8)$$

With τ_μ = characteristic time of the μ^{th} Kelvin-Voigt's chains
C_μ = μ^{th} spring of the multiple Kelvin-Voigt's chains
η_μ = μ^{th} dashpot of the multiple Kelvin-Voigt's chains
t_{0i} = time when the plateau are reached for the i^{th} cycle

Parameter τ_1 in Equation (6) is supposed constant for each cycle and has to be adapted for the best fit. Figure 16 shows the very good agreement between the modeling of the creep function and the experimental data. A value of 15 seconds was considered for parameter τ_1.

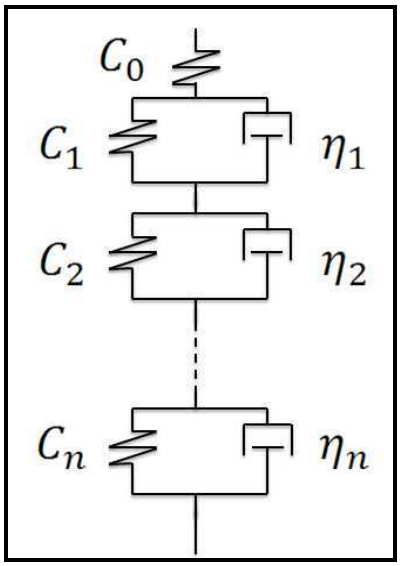

Figure 15 - Multiple Kelvin-Voigt's chains

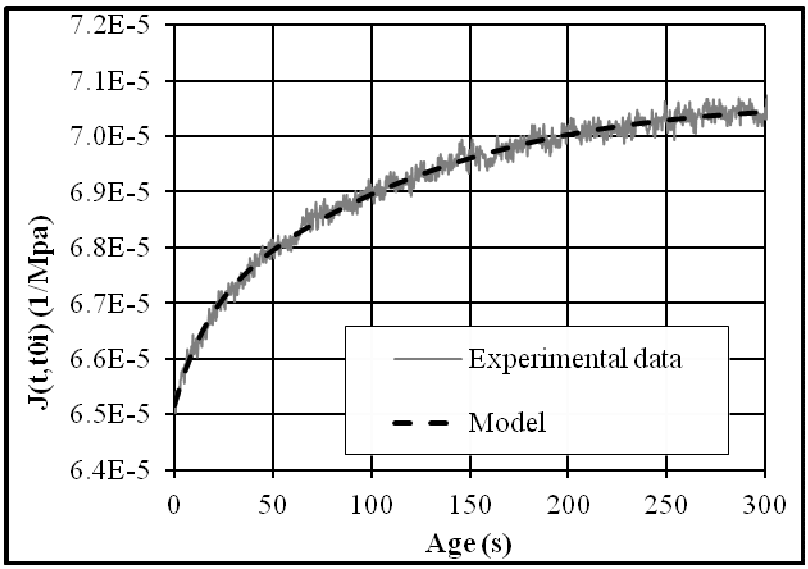

Figure 16 - Creep function modeling with multiple Kelvin-Voigt's chains model

As for the relaxation function, the creep function curves for each cycle can be normalized by the value reached at the end of the plateau and superimposed for looking at the evolution of the kinetics in function of the time. In order to do this, all creep curves normalized for the cycle carried out in tension are plotted in Figure 17. The standard deviation of all these creep curves is very low, what shows that for short durations of loadings (5 mn), the kinetics of the creep in tension are independent of the time at early age. The mean values of the normalized relaxation evolution in tension and in compression and of normalized creep evolution in tension are plotted in Figure 18. The 3 curves are perfectly

superimposed. In part 1, the same observation has been noticed for the normalized creep evolution in compression and the normalized relaxation evolution in compression. For short durations (5mn) and limited levels of loadings (20 % in compression and 40 % in tension), the kinetics of the creep and the relaxation in tension and in compression at early age are similar.

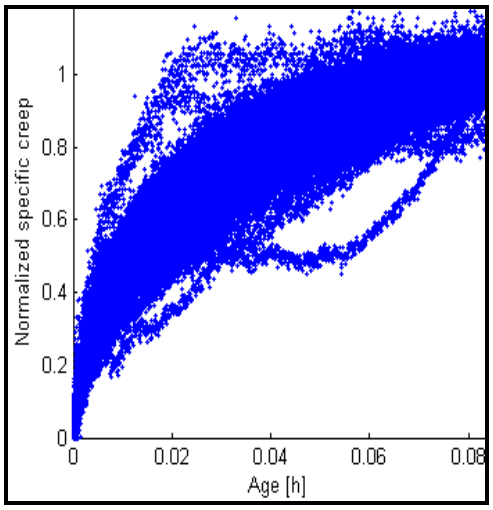

Figure 17 – The specific creeps are normalized by their value at 5 mn.

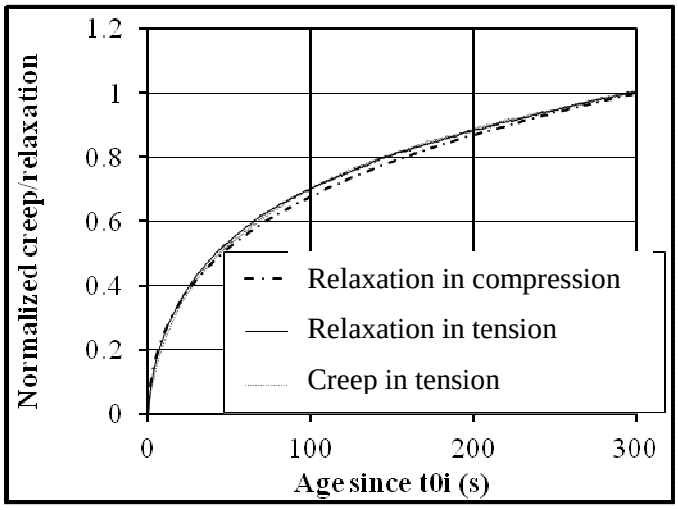

Figure 18 - Mean values of the normalized relaxation in tension and compression and the normalized creep in tension fitted by rheological model.

3.3. Creep recovery

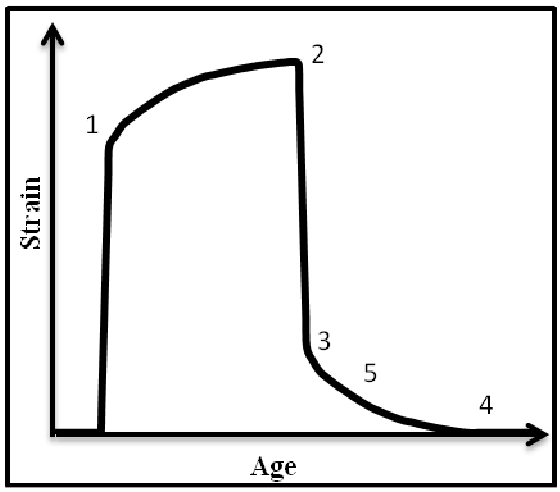

Figure 19 – typical creep cycle in tension

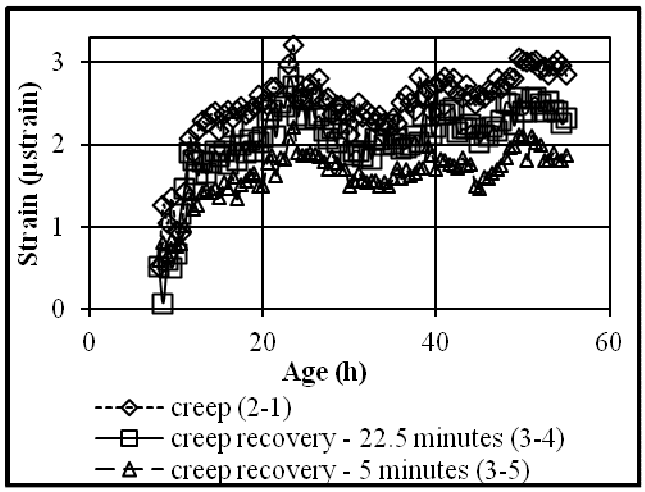

Figure 20 – Creep strain and creep recovery strain for each cycle

The visco-elastic properties of concrete at early age for short durations of loadings and limited stress strength ratio (40 % in tension) have been investigated by a comparison between the creep part and the creep recovery part for each cycle in tension. Figure 19 and Figure 20 show for each cycle the decomposition in several parts of the recorded strains, the creep strain (between 2 and 1) until the end of the plateau, the creep recovery at 5 mn after a total unloading (between 3 and 5) and the creep recovery at 22.5 mn after a total unloading (between 3 and 4). After 5 mn, a significant part of the creep strain is recovered and after 22.5 mn almost all creep strain is recovered. The creep recovery is a slower phenomenon than the creep. The very low difference between creep recovery strain at 22.5 mn and creep strain shows that this kind of loading induces no irreversibility in the concrete strain (Figure 20).

4. Conclusion

A revisited TSTM for the study of the restrained shrinkage of a concrete at early age is used for the monitoring of cyclic and short creeps and relaxations in tension and in compression since setting time. The cycle duration is approximate 30 mn. The creep or the relaxation duration is 5 mn. The loading consists in applying a constant stress strength ratio for each cycle.

The kinetics are not only the same for each cycle of a given test but are also the same for creep and relaxation tests in tension and in compression. This conclusion is however limited to early age concrete and for short durations and limited levels of loadings (20 % in compression and 40 % in tension).

A next step of this research is the study of the amplitude of the creep and the relaxation.

The creep recovery is slower than the creep phenomenon. However at early age and for short durations of loadings, the creep strain is relatively rapidly totally recovered in case of total unloading.

An excellent agreement between the experimental data has been obtained with the BTJASPE and the TSTM device. What is validated the credibility of the results and the protocols of loadings with both devices.

More sophisticated tests with more complex histories of loadings (various plateau durations) are still needed for computational purposes. The measurement of transversal displacement is also needed for future studies.

Another protocol can also be used in the future for the relaxation test. After the end of the plateau of deformation, the deformations could be imposed null instead of coming back to a null force.

Acknowledgements

Special thanks are addressed to Pierre Baesens and Jérôme Carette, from Université Libre de Bruxelles, BATir Department, who worked on the different tests.

References

[1] Slowik, V., Schmidt, D., Nietner, L., "Effect of stress relaxation on thermal stresses", Concreep 7, 2005, Nantes, France, pp.411-416

[2] Darquennes, A., Staquet, S., Espion, B., « Testing concrete at early age under restraint conditions in a tstm system », 13th International Conference Structural Fault & Repair, 15-17/6/2010. Proceedings CD ROM (M. FORDE, editor) Engineering Technics Press, Edinburgh, U.K., 11 pp., ISBN 0-947644-66-0; p.98 (Book of Abstracts)

[3] Darquennes, A., Staquet, S., Delplancke, M.-P., Espion B., Effect of autogenous deformation on the cracking risk of slag cement concretes. Cement and Concrete Composites. Volume 33, Issue 3, March 2011, pages 368-379.

[4] Darquennes, A., Staquet, S., Espion, B., "Determination of time-zero and its effect on autogenous deformation evolution", European Journal of Environmental and Civil Engineering, 15, 2011, pp 1017-1029.

[5] Boulay C., Merliot E., Staquet S., Marzouk O., Monitoring of the concrete setting with an automatic method, 13th International Conference Structural Faults & Repair - 2010, Edinburgh, 15-17/6/2010. Proceedings CD ROM (M. FORDE, editor), Engineering Technics Press, Edinburgh, U.K., 11 pp., ISBN 0-947644-67-9. (Book of Abstracts: ISBN 0-947644-66-0; p.98).

[6] Robeyst, N.,Gruyaert, E., Grosse, C.U.,De Belie, N., Monitoring the setting of concrete containing blast-furnace slag by measuring the ultrasonic p-wave velocity, Cement and Concrete Research, 38, 2008, pp 1169–1176.

[7] Bazant, Z.P.,Asghari, A., "Computation of Age-Dependent Relaxation spectra", Cement and Concrete Research, Vol. 4, No. 4 (1974).

[8] Bazant, Z.P., Wu, S.T., "Dirichlet Series Creep Functionfor Aging Concrete", J. Engng. Mech. Div., Proc. Am. Soc. Of Civil Engrs. 99, 367-387 (1973).

Monitoring of the creep and the relaxation behaviour of concrete since setting time, part 2 : tension

SSCS 2012 Numerical Modeling Strategies for Sustainable Concrete Structures
Aix-en-Provence, France
May 29-June 1, 2012

B. Delsaute[1], S. Staquet[1], C. Boulay[2]

[1]*ULB (Université Libre de Bruxelles), BATir Department – Brussels, Belgium*
[2] *IFSTTAR-Paris, Paris East University, France*

1. Introduction

Nowadays, the construction phases of modern concrete structures become more and more complex. Consequently, it is important to have a knowledge in depth of the early age behaviour of concrete, what will influence all the service life of the concrete structures. Even though the mechanical behaviour of hardened concrete can usually be correctly predicted; it is not always the case for the early age behaviour of concrete, when the mechanical properties change rapidly in function of the advancement of the hydration reaction. Among all the usual parameters (strengths, E-modulus…) needed for the design of the concrete structures, creep and relaxation in tension and in compression must also be taken into account. For example, in the design of a concrete dam, Slowik [1] showed that at early age, the relaxation phenomenon was responsible for a decrease of 70% of the thermally induced stresses in the structure.

A partnership between IFSTTAR and ULB allowed joined experimental tests on the same ordinary concrete in order to investigate the early age mechanical behaviour since setting time. Besides the usual determination of the instantaneous mechanical properties, this paper (part 1 & 2) presents an experimental methodology using two different test rigs enabling a monitoring of the stiffness, the creep or the relaxation of a concrete sample since setting time. Tension and compressive tests have been carried out on a revisited Temperature Stress Testing Machine (TSTM) at ULB [2][3] and are mainly presented in this part while compressive tests, carried out on another test rig called BTJASPE designed at IFSTTAR, have been presented in the first part.

A revisited TSTM system was developed in the laboratory of civil engineering at ULB for testing concrete in tension or in compression since setting time under free and restraint conditions. The TSTM consists of an electromechanical testing setup, where one end of the specimen is restrained by a steel head and the displacement of the other end is controlled by a motor moving the other steel head. The shape of the mould is a dog-bone. The Young's modulus, the creep or the relaxation of the sample can be monitored at early age by means of automatic cyclic loadings applied at regular intervals in tension or in compression. As in addition to the creep and elastic deformations, thermal and shrinkage deformations must also be known, a dummy mould was realized for the measurement of the thermal and free shrinkage deformations. A thermal regulation allowing the control of the sample's temperature was included in the revisited TSTM system as well as a couple of displacement sensors without contact allowing the start of the measurement since setting time.

For all the tests, rheological models are used for the description of the experimental set of data. In addition to the presentation of the results obtained in tension, the purpose of this part is to discuss the question of the equivalence between the early age creep and relaxation behaviour of concrete in tension and in compression for a typical ordinary concrete under isothermal (20°C) and sealed conditions. Finally, the creep recovery in tension is studied and discussed.

2. Test setup

2.1. Tested concrete description

The mixture proportions of the ordinary concrete under focus are given in Table 1. The water to cement ratio is equal to 0.54. More information about mechanical properties is given in part 1.

.

Components	Mass (kg /m^3)
CEMI 52.5 N PMES CP2	340
Sand (Bernières 0/4)	739
Gravel (Bernières 8/22)	1072
Total water	184

Table 1 - Mixture proportions of the concrete

2.2. Experimental tools

A revisited TSTM system was developed (since 2006) in the laboratory of civil engineering at the ULB for testing concrete since setting time under free and restraint conditions. For this purpose, a testing machine, a Walter+Bay LFMZ 400 kN electromechanical testing setup, has been revisited. The machine is totally programmable and controlled (force and displacement of each sensor) by computer. The machine is composed by a fixed steel head, a central unidimensional part and a moving end (Figure 2). The moving end is controlled by a motor moving the steel head. The transition area between the ends and the central part is characterized by a rounded shape in order to minimize a possible stress concentration and the risk of premature cracking in this zone. In the central part where the measurements of the displacements are taken, the stress field is assumed to be homogenous.

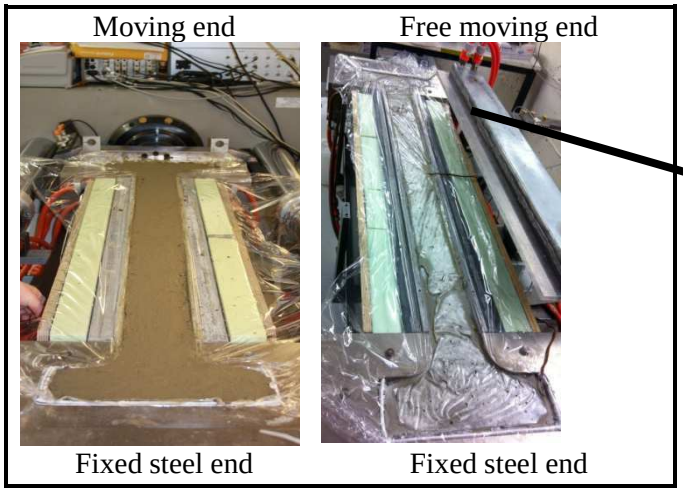

Figure 2 – a couple of moulds with different boundary conditions

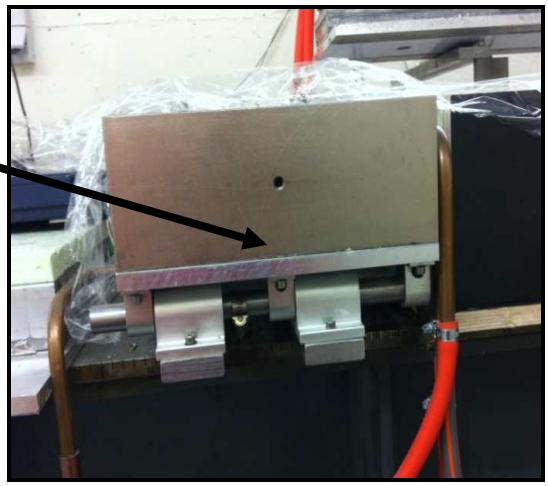

Figure 1 – Dummy mould : free moving end thanks to ball bearings

In addition to the creep and elastic deformations, thermal and shrinkage deformation must also be known. For this purpose, a dummy mould was realized for the measurement of the thermal and free shrinkage deformations. This mould has exactly the same geometry as the first one. The only difference is the total free movement of one of the ends (Figure 1).

The shape of the mould is a dog-bone. The dimensions of the cross section are 100x100 mm² in the central part and 300x100 mm² at the ends. The total length of the straight part is 1000 mm. With these dimensions, it is possible to realize tests for concrete with a maximal aggregate size of 20 mm. The fresh concrete is cast inside the mould up to a level of 100 mm. One T type thermocouple is placed in the middle of the sample during the casting, at each end and at mi-length of the central part of the mould. The temperature of the sample is controlled by a flow of a specific liquid for thermal

regulation circulating on all the sides of the specimen. A plastic sheet is placed, before casting, in the mould to ensure sealed conditions. Moreover, the plastic sheet helps also to reduce, with the presence of Teflon, the friction between the sample and the mould. The walls of the mould are made of aluminum (Figure 3) which was chosen for its high thermal conductivity (237 W/m.K) and its low density (2700 kg/m³). The deflection of the mould is very limited (+/-2mm) and the isothermal conditions are ensured thanks to a fast heat transfer with the zinc boxes. A specific liquid for thermal regulation flows inside zinc boxes beams which are placed all around the central part and on the ends and under them. Each box is independent and has its own water input and output system. A thermal insulation limits exchanges with the ambient environment. The equipment is located in an air-conditioned room with a control system of the temperature and the humidity.

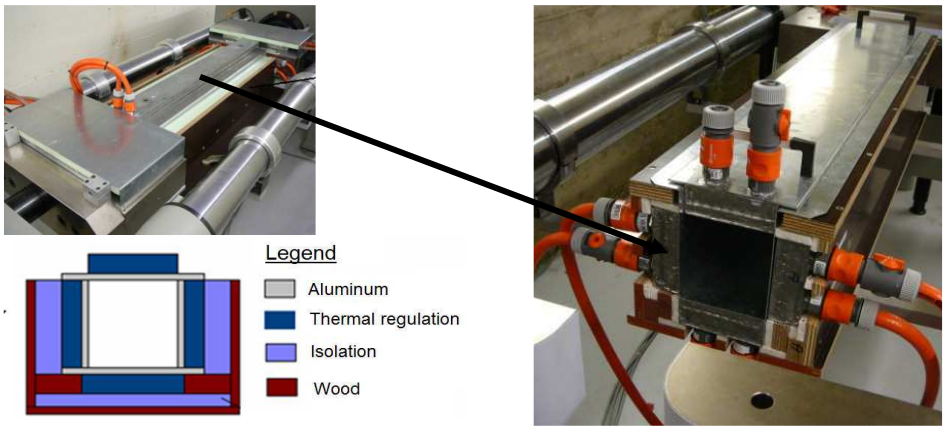

Figure 3 - Thermal insulation

Displacements in the central part are recorded by Foucault current's sensors (contact free sensors). Sensors have an accuracy of 0.014 µm. The displacement sensors of displacement are placed on invar supports which are fixed on a rigid frame made of steel bars externally supported by the TSTM (Figure 4). The distance between both sensors is 750 mm (where the stress field is homogeneous in the sample). Invar rods are anchored in the concrete at a depth of 50 mm. The link between the concrete displacement and the sensor is then assured. These invar rods are characterized by a low dilatation coefficient limiting the effect of ambient temperature on the deformations measurement. They are kept in their initial position thanks to a brass ring before the beginning of the test. These sensors have two advantages. Firstly, the absence of contact between the sensors and the mould avoids measurement artifacts. Secondly, an instantaneous volt conversion in micrometer of the sensors allows piloting the TSTM system with the displacement directly measured in concrete.

Figure 4 - displacement sensors in the central part of the specimen

The horizontality of the TSTM device is an advantage for the efficiency of the casting. Moreover, sensors are well anchored at mid-height and not in the superficial layer of the sample, what could have induced an error by a possible different mechanical behavior between the core layer and the superficial layer characterized by a lower density in aggregates than the one of the core layer.

2.3. Protocol of loadings

The system is controlled in displacement (measured in the straight part of the concrete sample or at the end of the moving steel head) and in force. The direct measurement of the evolution of the Young's modulus, the creep and the relaxation can be carried out. The start of the tests has been choosen at the end of the setting time [4][5]. This time is determined thanks to a device called FreshCon allowing the determination of the setting time on basis of ultrasonic measurements [6].

2.3.1. Relaxation test

Figure 5 introduces the protocol of loadings for the study of the relaxation phenomena. Firstly, the sample is loaded. The Young's modulus measurement is done as follows: for every cycle of loading, the moving end is controlled by the displacement sensor at the end of the moving steel head and the increase of the loading. The increase of the loading is carried out at constant speed (between 1 and 5 µm/s), the value of the speed depends on the stiffness of the concrete, the concrete strength at the age of loading and the type of loading (compression or tension) because the sample is loaded at 20% of the strength/stress ratio in compression and at 40% of the strength/stress ratio in tension.

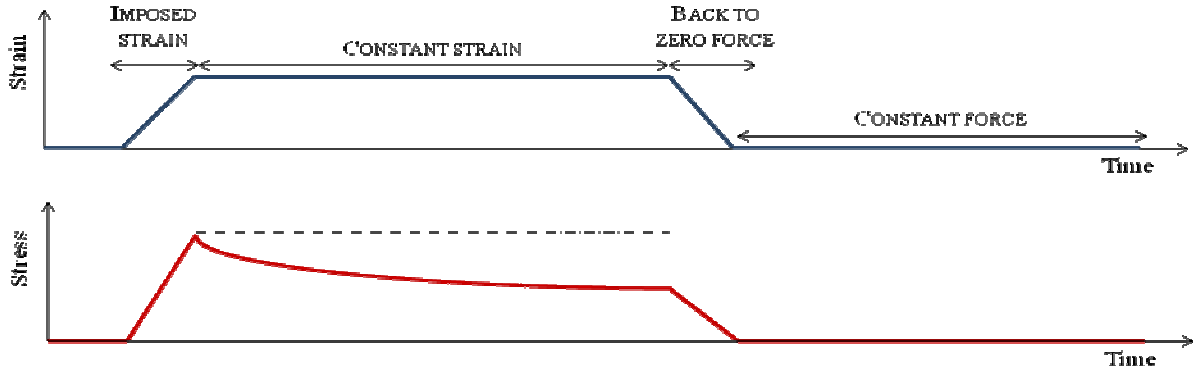

Figure 5 - relaxation cycle in tension

Secondly, a constant strain in the sample is imposed thanks to a real time subtraction between the strain of the specimen in the TSTM and the dummy specimen in the companion (passive) mould. The recorded displacements by sensors without contact are noted S1, S2 in the mould 1 (TSTM) and S3, S4 in the mould 2. The initial distance between the sensors is equal to 750 mm. It allows piloting the TSTM system on basis of the mechanical parameters excluding the free deformations due to thermal variations ε_{th} and due to shrinkage ε_{sh}. So, the direct measurement of the elastic ε_e and creep ε_c strains or the relaxation stresses is possible with the simultaneous use of the first and the second mould (Table 2).

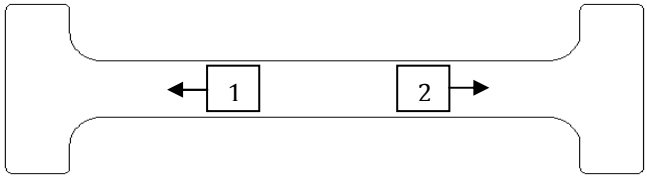	Mould 1: $\frac{S1+S2}{750\ mm} = \varepsilon_e + \varepsilon_c + \varepsilon_{th} + \varepsilon_{sh}$
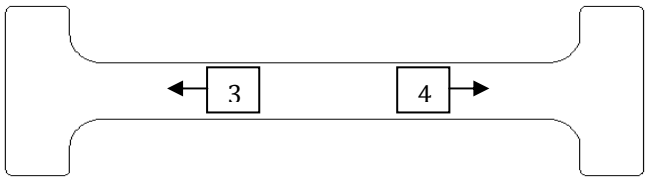	Mould 2: $\frac{S3+S4}{750\ mm} = \varepsilon_{th} + \varepsilon_{sh}$
TSTM device is controlled by (S1+S2)-(S3+S4) which corresponds to creep and elastic strains.	

Table 2 – Strain measurements for each mould

The sample is then unloaded and the moving end is moved backwards to a null force for a period of 24

mn. Recordings are taken during the cycles. The Young's modulus is computed from measurements taken in concrete in the straight part of the sample during each loading cycle. The strains in the straight part are not restraint by the shape and the walls of the mould (friction is supposed to be very low between Teflon® and plastic sheet). These displacement measurements can then be directly used to compute the Young's modulus. The stresses relaxation is computed during the plateau of deformation.

2.3.2. Creep test

Figure 6 introduces the protocol of loadings for the study of the creep phenomena. Firstly, the sample is loaded at 40% of the strength/stress ratio in tension as for the relaxation test in tension. Secondly, a constant force in the sample is imposed during 5 mn. The sample is then unloaded and the moving end is moved backwards to a null force for a period of 24 mn. Recordings are taken during the cycles. The Young's modulus is computed from measurements taken in concrete in the straight part of the sample during each loading cycle. The creep strain is computed during the plateau of force. The creep recovery is computed during the plateau at null force.

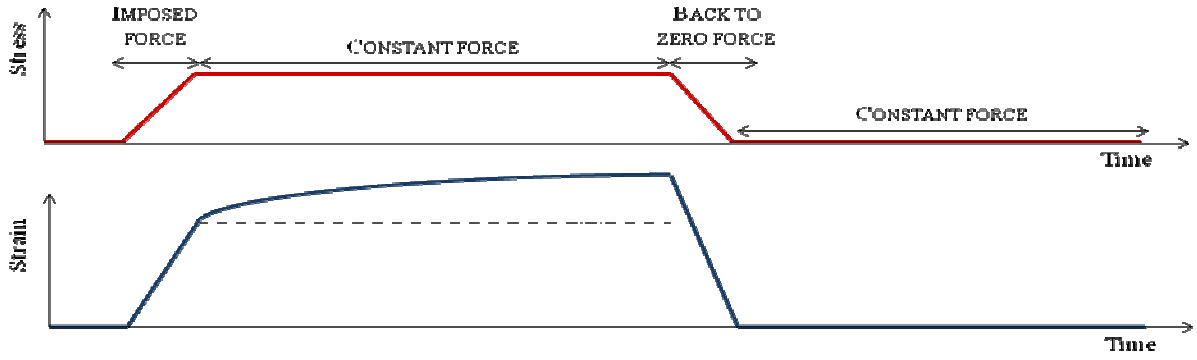

Figure 6 - creep cycle

3. Results and discussions

One tensile creep test and one relaxation test in tension and compression are presented here.

3.1. Relaxation test

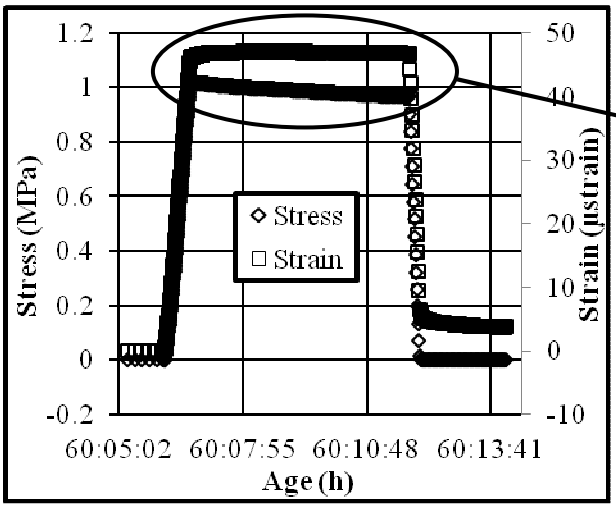

Figure 7 – Typical relaxation cycle in tension

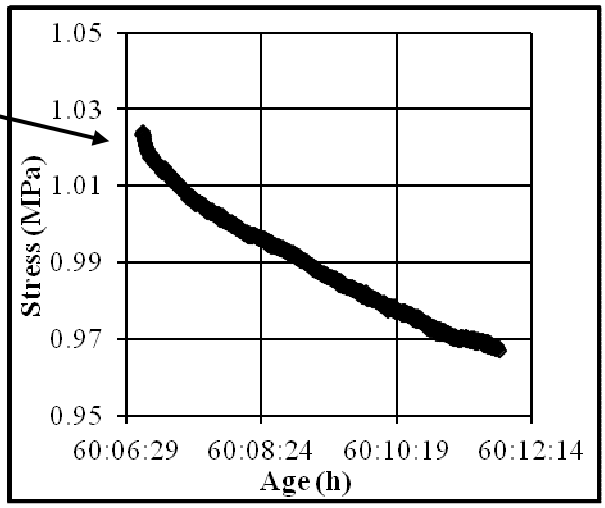

Figure 8 – Zoom on the relaxation stresses during one cycle

A typical relaxation record is presented in Figure 7 and Figure 8. The age of the concrete is called t. The stress evolution is measured continuously. At any cycle, named i, the relaxation is counted as soon as the plateau is reached; this moment is called t_{0i}. The stress $\sigma(t,t_{0i})$ is then recorded whereas a constant strain ε_{0i} is applied. The ratio in Equation 1 is defined as the stiffness. The specific relaxation R^* is defined as this stiffness diminished of the initial stiffness at t_{0i} (see Equation 2).

$$R(t,t_{0i}) = \frac{\sigma(t,t_{0i})}{\varepsilon_{0i}} \quad (1)$$

$$R^*(t,t_{0i}) = R(t,t_{0i}) - R(t_{0i},t_{0i}) = R(t,t_{0i}) - E(t_{0i}) \quad (2)$$

The whole test duration was 68 hours. The duration of each cycle is around 30 minutes. The loading is fixed to a value equal at any time to a percentage of 40 % of the tensile strength and to a percentage of 20 % of the compressive strength. Figure 9 shows an uniaxial rheological model, proposed by Bazant [7], which is used to fit the observed stiffness of each cycle (relaxation function).

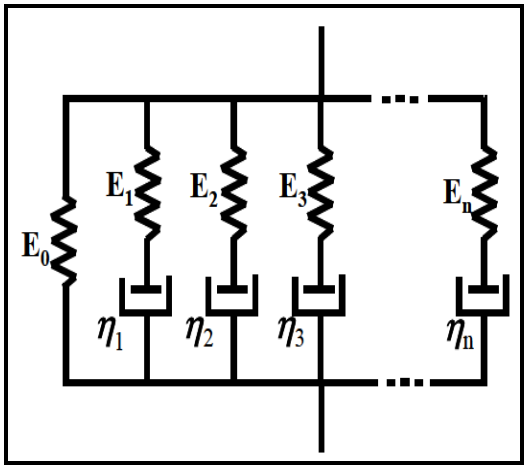

Figure 9 - Multiple Maxwell's chains

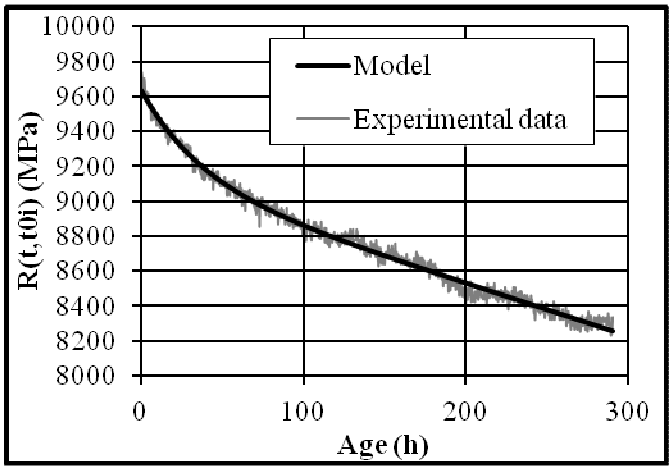

Figure 10 - Relaxation function modeling for the 5th cyle in tension with multiple Mawell's chains model

Relaxation function can be develop in Dirichlet's series expansion [7]:

$$R(t,t_{0i}) = E_0(t_{0i}) + \sum_{\mu=1}^{N} E_\mu(t_{0i}).e^{\frac{t_{0i}-t}{\tau_\mu}} \quad (3)$$

$$\tau_\mu = \tau_1.10^{1-\mu} \ (\mu = 1, \ldots, N) \quad (4)$$

$$\eta_\mu(t) = \tau_\mu.E_\mu(t) \quad (5)$$

With τ_μ= characteristic time
E_μ= μ^{th} spring of the multiple Maxwell's chains
η_μ= μ^{th} dashpot of the multiple Maxwell's chains
t_{0i}= time when the plateau is reached for the i^{th} cycle

The characteristic time τ_1 is supposed as constant and has to be optimized for the best fit. A value of 12 seconds was considered for τ_1. Three Maxwell's chains are used for the modeling of the experimental data of the relaxation test. The least and square method is used to define the value of the different parameters of the rheological model. Figure 10 shows the very good agreement between the modelling of the relaxation function and the experimental data.

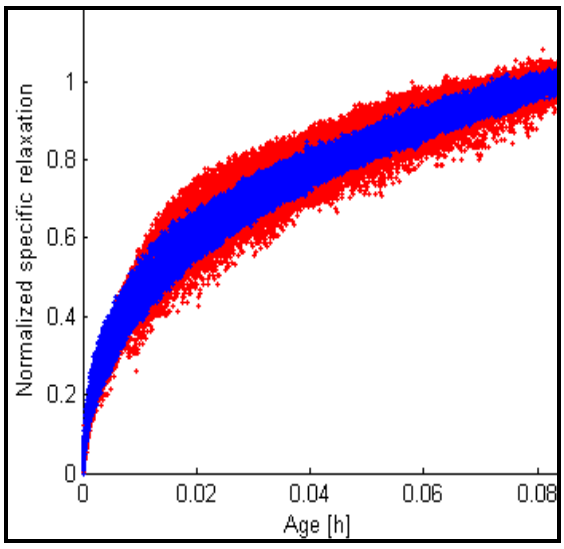

Figure 11 - The specific creeps are normalized by their value at 5 mn.

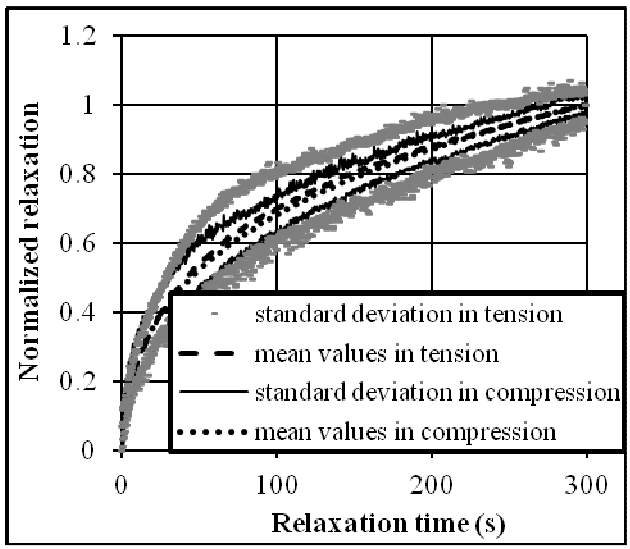

Figure 12 – Mean values of the normalized relaxation in tension and compression between +/- standard deviation fitted by rheological model.

As shown in part 1, the relaxation function or stiffness curves for each cycle can be normalized by the value reached at the end of the plateau and superimposed for looking at the evolution of the kinetics in function of the time. In order to do this, all stiffness curves normalized for the cycle carried out in tension and compression are plotted in Figure 11 . The standard deviation of all these relaxation curves is very low, what shows that the kinetics of the relaxation in tension and compression are independent of the time at early age. No significant difference between tensile and compressive relaxation curves can be observed. The mean values and the standard deviation in tension and in compression are plotted in the Figure 12. The deviations in tension are higher than those in compression because of the lack of accuracy of the measurements related to very small values of loadings applied in tension (ratio of 5 between compressive and tensile loadings) due to the presence of a noise on the measurements of very low amplitude. In part 1, results in compression are compared with another device (BTJASPE). It was shown that the results are perfectly superimposed and then validate the results for both machines. For short durations of loadings (5 mn) and low stress strength ratio, the kinetics of the relaxation in tension and in compression are similar.

3.2. Creep test

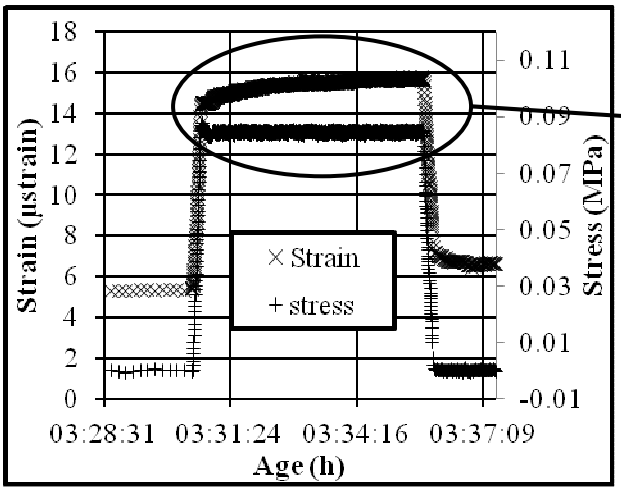

Figure 13 – Typical creep cycle

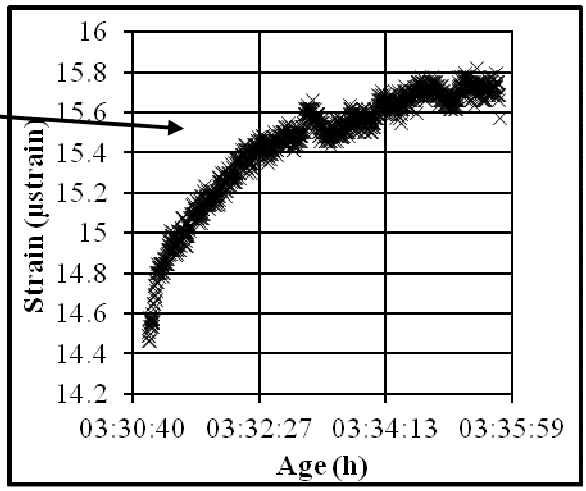

Figure 14 – Zoom on the creep strains during one cycle

A typical creep record is presented in Figure 13 and Figure 14. The sample strain, $\varepsilon(t)$ is measured continuously. At any cycle, named i, the creep is counted as soon as the plateau is reached. This moment is called t_{0i}.

The whole test duration was 72 hours. The duration of each cycle is around 30 minutes. The loading is fixed to a value equal to 40 % of the tensile strength and 20 % of the compressive strength. Figure 9 shows an uniaxial Dirichlet's creep model which is used to fit the observed relaxation data of each cycle. In case of creep, a multiple Kelvin-Voigt's chains (Figure 15) is used to fit the observed creep data of each cycle as it was suggested by Bazant [8]. The creep $J(t,t_{0i})$ can be computed for each cycle during the loading plateau. The mathematical resolution (Dirichlet's series expansion) of the rheological model gives the relation between the creep function and the different parameters of the rheological model (Equation 6).

$$J(t,t_{0i}) = \frac{1}{C_0(t_{0i})} + \sum_{i=\mu}^{N} \frac{1}{C_\mu(t_{0i})}\left(1 - e^{-\frac{t-t_{0i}}{\tau_\mu}}\right) \quad (6)$$

$$\tau_\mu = \tau_1 . 10^{1-\mu} \ (\mu = 1, \ldots, N) \quad (7)$$

$$\eta_\mu(t) = \tau_\mu . E_\mu(t) \quad (8)$$

With τ_μ = characteristic time of the μ^{th} Kelvin-Voigt's chains
C_μ = μ^{th} spring of the multiple Kelvin-Voigt's chains
η_μ = μ^{th} dashpot of the multiple Kelvin-Voigt's chains
t_{0i} = time when the plateau are reached for the i^{th} cycle

Parameter τ_1 in Equation (6) is supposed constant for each cycle and has to be adapted for the best fit. Figure 16 shows the very good agreement between the modeling of the creep function and the experimental data. A value of 15 seconds was considered for parameter τ_1.

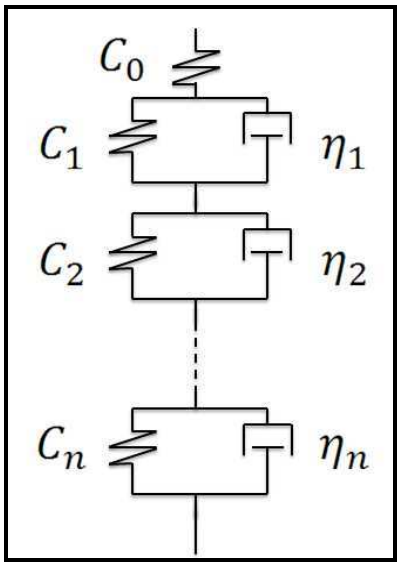

Figure 15 - Multiple Kelvin-Voigt's chains

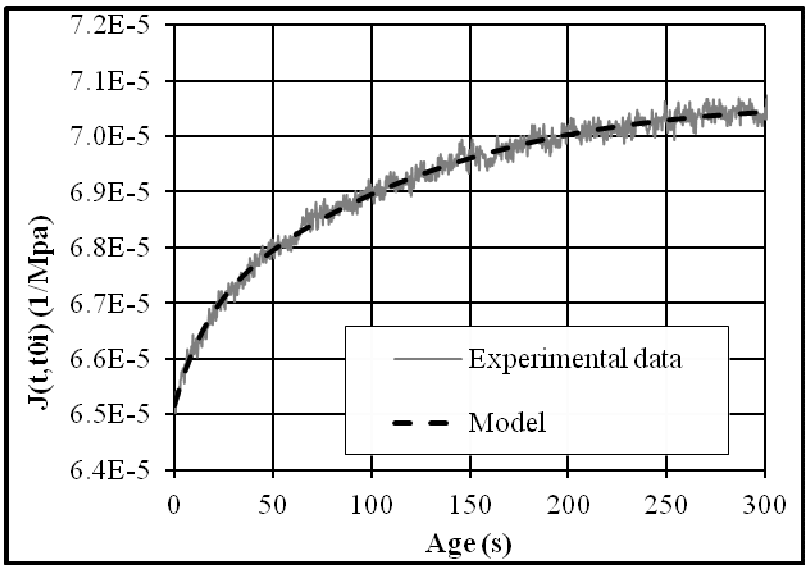

Figure 16 - Creep function modeling with multiple Kelvin-Voigt's chains model

As for the relaxation function, the creep function curves for each cycle can be normalized by the value reached at the end of the plateau and superimposed for looking at the evolution of the kinetics in function of the time. In order to do this, all creep curves normalized for the cycle carried out in tension are plotted in Figure 17. The standard deviation of all these creep curves is very low, what shows that for short durations of loadings (5 mn), the kinetics of the creep in tension are independent of the time at early age. The mean values of the normalized relaxation evolution in tension and in compression and of normalized creep evolution in tension are plotted in Figure 18. The 3 curves are perfectly

superimposed. In part 1, the same observation has been noticed for the normalized creep evolution in compression and the normalized relaxation evolution in compression. For short durations (5mn) and limited levels of loadings (20 % in compression and 40 % in tension), the kinetics of the creep and the relaxation in tension and in compression at early age are similar.

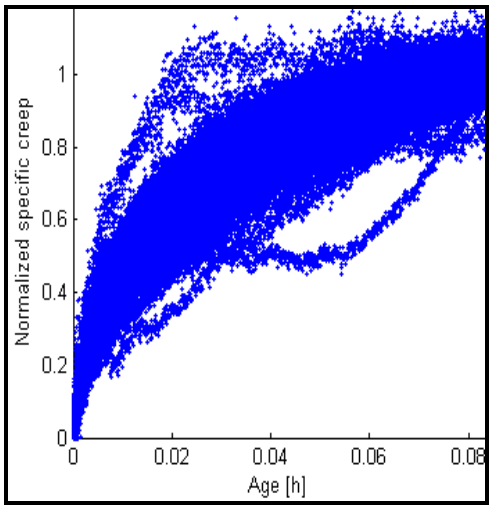

Figure 17 – The specific creeps are normalized by their value at 5 mn.

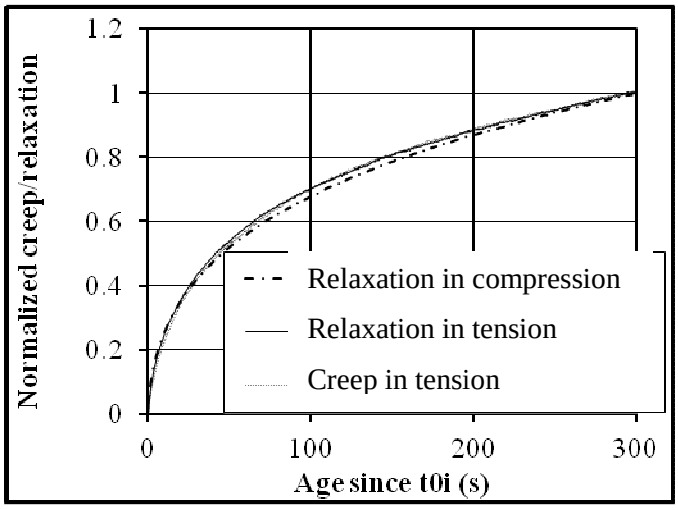

Figure 18 - Mean values of the normalized relaxation in tension and compression and the normalized creep in tension fitted by rheological model.

3.3. Creep recovery

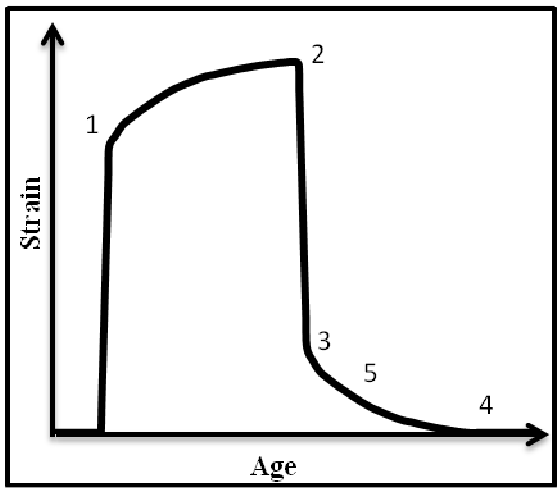

Figure 19 – typical creep cycle in tension

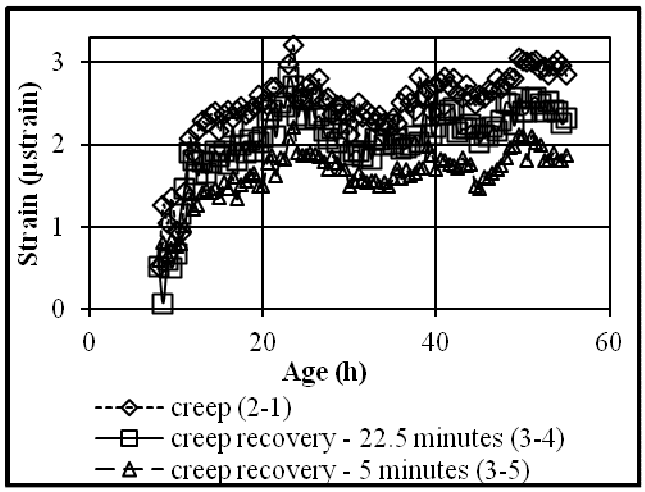

Figure 20 – Creep strain and creep recovery strain for each cycle

The visco-elastic properties of concrete at early age for short durations of loadings and limited stress strength ratio (40 % in tension) have been investigated by a comparison between the creep part and the creep recovery part for each cycle in tension. Figure 19 and Figure 20 show for each cycle the decomposition in several parts of the recorded strains, the creep strain (between 2 and 1) until the end of the plateau, the creep recovery at 5 mn after a total unloading (between 3 and 5) and the creep recovery at 22.5 mn after a total unloading (between 3 and 4). After 5 mn, a significant part of the creep strain is recovered and after 22.5 mn almost all creep strain is recovered. The creep recovery is a slower phenomenon than the creep. The very low difference between creep recovery strain at 22.5 mn and creep strain shows that this kind of loading induces no irreversibility in the concrete strain (Figure 20).

4. Conclusion

A revisited TSTM for the study of the restrained shrinkage of a concrete at early age is used for the monitoring of cyclic and short creeps and relaxations in tension and in compression since setting time. The cycle duration is approximate 30 mn. The creep or the relaxation duration is 5 mn. The loading consists in applying a constant stress strength ratio for each cycle.

The kinetics are not only the same for each cycle of a given test but are also the same for creep and relaxation tests in tension and in compression. This conclusion is however limited to early age concrete and for short durations and limited levels of loadings (20 % in compression and 40 % in tension).

A next step of this research is the study of the amplitude of the creep and the relaxation.

The creep recovery is slower than the creep phenomenon. However at early age and for short durations of loadings, the creep strain is relatively rapidly totally recovered in case of total unloading.

An excellent agreement between the experimental data has been obtained with the BTJASPE and the TSTM device. What is validated the credibility of the results and the protocols of loadings with both devices.

More sophisticated tests with more complex histories of loadings (various plateau durations) are still needed for computational purposes. The measurement of transversal displacement is also needed for future studies.

Another protocol can also be used in the future for the relaxation test. After the end of the plateau of deformation, the deformations could be imposed null instead of coming back to a null force.

Acknowledgements

Special thanks are addressed to Pierre Baesens and Jérôme Carette, from Université Libre de Bruxelles, BATir Department, who worked on the different tests.

References

[1] Slowik, V., Schmidt, D., Nietner, L., "Effect of stress relaxation on thermal stresses", Concreep 7, 2005, Nantes, France, pp.411-416

[2] Darquennes, A., Staquet, S., Espion, B., « Testing concrete at early age under restraint conditions in a tstm system », 13th International Conference Structural Fault & Repair, 15-17/6/2010. Proceedings CD ROM (M. FORDE, editor) Engineering Technics Press, Edinburgh, U.K., 11 pp., ISBN 0-947644-66-0; p.98 (Book of Abstracts)

[3] Darquennes, A., Staquet, S., Delplancke, M.-P., Espion B., Effect of autogenous deformation on the cracking risk of slag cement concretes. Cement and Concrete Composites. Volume 33, Issue 3, March 2011, pages 368-379.

[4] Darquennes, A., Staquet, S., Espion, B., "Determination of time-zero and its effect on autogenous deformation evolution", European Journal of Environmental and Civil Engineering, 15, 2011, pp 1017-1029.

[5] Boulay C., Merliot E., Staquet S., Marzouk O., Monitoring of the concrete setting with an automatic method, 13th International Conference Structural Faults & Repair - 2010, Edinburgh, 15-17/6/2010. Proceedings CD ROM (M. FORDE, editor), Engineering Technics Press, Edinburgh, U.K., 11 pp., ISBN 0-947644-67-9. (Book of Abstracts: ISBN 0-947644-66-0; p.98).

[6] Robeyst, N.,Gruyaert, E., Grosse, C.U.,De Belie, N., Monitoring the setting of concrete containing blast-furnace slag by measuring the ultrasonic p-wave velocity, Cement and Concrete Research, 38, 2008, pp 1169–1176.

[7] Bazant, Z.P.,Asghari, A., "Computation of Age-Dependent Relaxation spectra", Cement and Concrete Research, Vol. 4, No. 4 (1974).

[8] Bazant, Z.P., Wu, S.T., "Dirichlet Series Creep Functionfor Aging Concrete", J. Engng. Mech. Div., Proc. Am. Soc. Of Civil Engrs. 99, 367-387 (1973).